Modulation of potassium channel function confers a hyperproliferative invasive phenotype on embryonic stem cells

Junji Morokuma*, Douglas Blackiston*, Dany S. Adams*, Guiscard Seebohm[†‡], Barry Trimmer[§], and Michael Levin*[¶]

*Center for Regenerative and Developmental Biology, Forsyth Institute, and Department of Developmental Biology, Harvard School of Dental Medicine, 140 The Fenway, Boston, MA 02115; [†]Institute of Physiology I, University of Tubingen, 72076 Tubingen, Germany; [‡]Biochemistry I, Ruhr University Bochum, 44780 Bochum, Germany; and [§]Department of Biology, Tufts University, Medford, MA 02155

Communicated by Clifford J. Tabin, Harvard Medical School, Boston, MA, August 22, 2008 (received for review February 5, 2008)

Ion transporters, and the resulting voltage gradients and electric fields, have been implicated in embryonic development and regeneration. These biophysical signals are key physiological aspects of the microenvironment that epigenetically regulate stem and tumor cell behavior. Here, we identify a previously unrecognized function for KCNQ1, a potassium channel known to be involved in human Romano–Ward and Jervell–Lange–Nielsen syndromes when mutated. Misexpression of its modulatory wild-type β-subunit XKCNE1 in the *Xenopus* embryo resulted in a striking alteration of the behavior of one type of embryonic stem cell: the pigment cell lineage of the neural crest. Depolarization of embryonic cells by misexpression of KCNE1 non-cell-autonomously induced melanocytes to overproliferate, spread out, and become highly invasive of blood vessels, liver, gut, and neural tube, leading to a deeply hyperpigmented phenotype. This effect is mediated by the up-regulation of *Sox10* and *Slug* genes, thus linking alterations in ion channel function to the control of migration, shape, and mitosis rates during embryonic morphogenesis. Taken together, these data identify a role for the KCNQ1 channel in regulating key cell behaviors and reveal the molecular identity of a biophysical switch, by means of which neoplastic-like properties can be conferred upon a specific embryonic stem cell subpopulation.

cancer | ion channel | melanocyte | neural crest | KCNQ

Embryonic stem cells' behavior is controlled in part by signals from their environment. It is now clear that ion currents, electric fields, and endogenous voltage gradients are an endogenous system for cellular communication (1, 2). Roles for bioelectric signals have been uncovered in galvanotaxis of migratory cells, mitotic regulation, and control of differentiation, as well as in complex morphogenetic events, such as wound healing, limb development, left–right patterning, neurogenesis, vertebrate tail regeneration, and cancer (3–8).

Stem cells have distinguishing electrophysiological properties (9–11) and express a variety of passive (12, 13) and active (14) electrogenic transporters. Membrane hyperpolarization triggers, and is required for, myogenin and MEF-2 expression in myoblast differentiation (15), whereas direct electrical modulation of cells can result in a dedifferentiation phenotype (16, 17), raising the possibility that depolarization of cells may move them toward a more primitive, stem-like state.

The functional significance of electrical signals for stem cells' participation in complex morphogenetic events is largely mysterious. Likewise, the proximal transcriptional targets that link bioelectrical events to changes in cell behavior remain unknown. Progress in this fascinating field requires identification of both the source and the downstream targets of ion flows in a well characterized embryonic stem cell population. Neural crest cells differentiate into a variety of cell types, including smooth muscle cells, peripheral neurons, glia, craniofacial cartilage and bone, and endocrine and pigment cells, playing key roles in morphogenesis of the face, heart, and other structures.

To contribute to basic developmental biology and regenerative medicine (seeking novel ways to rationally modulate the position, identity, and number of embryonic stem cells), we performed molecular and pharmacological screens (18, 19) for ion flows that regulate stem cell behavior during pattern formation. We uncovered a role for a channel in neural crest regulation: KCNQ1/KCNE1.

KCNQ1 (also known as KvLQT1 and Kv7.1) is a six-transmembrane-region K^+ channel. When coassembled with the regulatory accessory subunit KCNE1 (also known as minK and Isk), it forms the "slow delayed rectifier" (20, 21). Mutations in KCNQ are responsible for an inherited birth defect that leads to cardiac long-QT arrhythmia (22), and for the hearing loss observed in Jervell and Lange–Nielsen Syndromes (23).

We showed recently that the KCNQ1/KCNE1 channel functions in left–right patterning of early *Xenopus* embryos (24). Here, we demonstrate that manipulation of this channel activity in *Xenopus* embryos results in up-regulation of *Xslug*, and ultimately in a drastic increase in melanocyte proliferation, cell shape change, and induction of invasiveness in these neural crest derivatives. In addressing the control of embryonic stem cell behavior by ion transporters, our data reveal a biophysical mechanism that confers a neoplastic-like phenotype on a specific subpopulation of embryonic stem cells.

Results

KCNE1 Misexpression Induces Hyperpigmentation. KCNQ1 but not KCNE1 is normally expressed in the neural crest in *Xenopus* embryos [supporting information (SI) Figs. S1 and S2]. Microinjection of mRNA encoding wild-type KCNE1 into one-cell frog embryos resulted in a striking hyperpigmentation observed in 32% of KCNE1-injected larvae by stage 45 (Fig. 1). Misexpression of other ion transporters, including Bir10, H,K-ATPase, ROMK, and Mirp2, did not cause hyperpigmentation ($n > 100$ for each).

Quantification of melanocyte number and total melanin content (Table 1) revealed a 2.1-fold increase in the number of pigment cells per unit area after KCNE1 misexpression. However, KCNE1-injected larvae had only 1.4-fold the melanin of control embryos, demonstrating that the hyperpigmentation effect is not due to greater pigment content per cell but is completely accounted for by the increase in melanocyte number. This hyperproliferation of melanocytes was not accompanied by general disruptions of morphogenesis, twinning, or axial duplications; the KCNE1-overexpressing larvae had normal dorsoanterior index, correct

Author contributions: J.M., D.B., D.S.A., G.S., and M.L. designed research; J.M., D.B., D.S.A., G.S., B.T., and M.L. performed research; J.M., D.S.A., G.S., and B.T. contributed new reagents/analytic tools; J.M., D.B., D.S.A., G.S., and B.T. analyzed data; and J.M., D.B., D.S.A., G.S., and M.L. wrote the paper.

The authors declare no conflict of interest.

[¶]To whom correspondence should be addressed. E-mail: mlevin@forsyth.org.

This article contains supporting information online at www.pnas.org/cgi/content/full/0808328105/DCSupplemental.

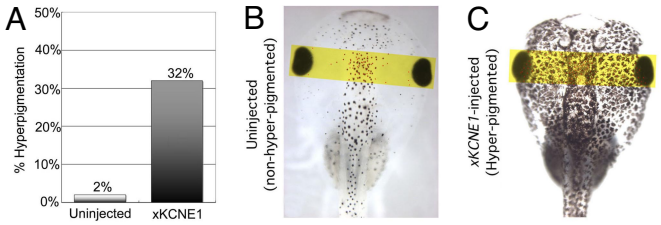

Fig. 1. KCNE1 overexpression induces hyperpigmentation. (*A*) Microinjection of KCNE1 mRNA at the one-cell stage induces 32% of embryos grown to stage 45 to exhibit hyperpigmentation compared with controls (<2%). (*B*) Controls. (*C*) Hyperpigmented embryos have far more melanocytes in the head but very normal overall development. Yellow rectangle indicates region in which melanocytes were counted (Table 1). (Magnifications: *B* and *C*, ×9.)

length and proportions, and proper patterning of eyes, heart, and face ($n > 500$; examples shown in Figs. 1 *B* and *C* and 4*A*, and Figs. S3 and S8 *A* and *B*). We conclude that misexpression of KCNE1 specifically increases the production of melanocytes.

KCNE1 Misexpression Depolarizes Embryonic Cells by Inhibition of KCNQ1. We next asked whether the effect of KCNE1 was mediated by modulation of endogenous KCNQ1 channels. In many cell types, including some neurons and nonexcitable tissues, KCNQ1 channels help determine resting membrane potential (25, 26). The average potential of *Xenopus* embryonic cells in the KCNQ1-expressing region is −21.6 mV (Fig. S4*A*). This is similar to the transmembrane potential in oocytes (−20 to −35 mV), allowing us to examine the effects of KCNE1 expression on KCNQ1 currents directly by electrophysiology. KCNQ1 expression in *Xenopus* oocytes resulted in a rapidly activating, voltage-dependent, and K^+-selective channel; this results in a hyperpolarization of the resting membrane potential that can be rescued by inhibition with the KCNQ1 blocker Chromanol 293B (Fig. S4 *B–D*). These data suggest that at resting potentials similar to those found during neural crest induction, KCNQ1 channels contribute significantly to membrane voltage.

Coexpression with KCNE1 reduced KCNQ1 currents at a wide range of transmembrane potentials (Fig. 2*A* and Fig. S5). Biotinylation Western blot analysis (Fig. 2*B*) supported a direct effect of the KCNE1 protein on the KCNQ1 channel (not on localization of channels to the plasma membrane). We conclude that coexpression of KCNE1 inhibits the activity of the hyperpolarizing KCNQ1 independent of trafficking to the cell surface.

Exposure at stage 41 to Chromanol 293B, a specific blocker of KCNQ1 (27), also resulted in hyperpigmentation (Fig. S3), consistent with inhibition of KCNQ1 being responsible for hyperpigmentation. The physiology data showing reduction of KCNQ1 currents by KCNE1, together with the observation that the same embryonic phenotype is obtained by direct KCNQ1 blockade as by KCNE1 misexpression, suggest that the induction of hyperpigmentation by KCNE1 is mediated by reduction of KCNQ1 activity.

Table 1. Hyperpigmentation phenotype

Measurement	Controls	*XKCNE1* mRNA	Fold increase
Hyperpigmentation incidence, %	2 (n = 714)	32 (n = 304)	16
Pigment cell count in eye area (n = 5)	67.2 ± 5.1	146.2 ± 6.1	2.1
Melanin content in whole embryo, A_{414} (n = 5)	0.176	0.255	1.4

Embryos at the one-cell stage were injected with synthetic mRNA encoding wild-type *Xenopus laevis* KCNE1 protein. Although embryos injected with β-gal mRNA (negative control) exhibited only the normal 2% background of hyperpigmentation, misexpression of KCNE1 caused 32% of the embryos to develop a hyperpigmented phenotype ($P < 0.01$). A rectangular area was defined in each larva at stage 45, and the number of melanocytes was counted, revealing that KCNE1-injected larvae exhibited 2.1 times more melanocytes in that region compared with controls. Injected larvae had only 1.4 times more total melanin. The effect is dose-dependent; when the amount of injected KCNE1 mRNA was cut 50%, the percentage of hyperpigmented larvae dropped by 30% (n = 887), but the degree of hyperpigmentation in each affected individual did not change appreciably.

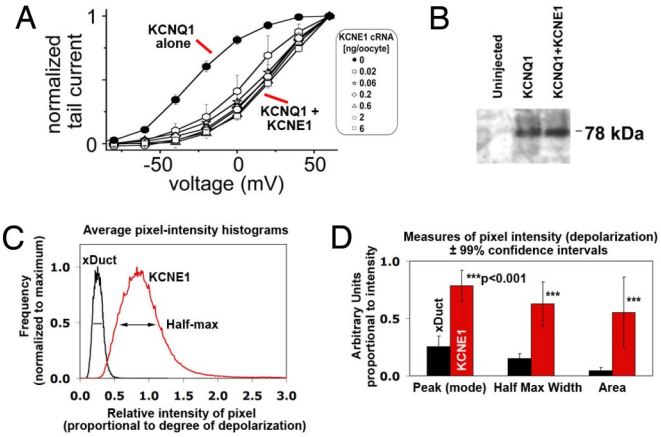

Fig. 2. KCNE1 inhibits KCNQ1 currents and depolarizes embryonic cells. (*A*) Tail currents were analyzed at −120 mV and normalized to the value followed after the 60-mV depolarizing pulse to estimate the voltage dependence of channel activation (n = 10 or 11). At voltages of 0 mV or less, addition of KCNE1 reduced the currents compared with KCNQ1 alone. (*B*) KCNQ1 (5 ng of mRNA) was expressed alone or together with 0.2 ng of KCNE1 mRNA. Each lane was loaded with equal amounts of protein (as estimated by Bradford test and Ponceau staining). Four consecutive biotinylation Western blots detected no clear alterations of KCNQ1 protein in the plasma membrane (densitometric analysis of all four gels normalized to the respective KCNQ1 band gave 1.0061 ± 0.1025 for KCNQ1 + KCNE1 injections). Analysis of membrane potential *in vivo* using DiSBAC voltage reporter dye reveals that KCNE1 mRNA expression depolarizes cells in the neurulating embryo. (*C*) Histograms showing normalized frequencies corresponding to normalized fluorescence intensities were created for each embryo (n = 37). One example each of the histograms from controls (injected with mRNA encoding *Xenopus* Ductin, a subunit of the V-ATPase ion pump) and KCNE1-injected embryos are shown. The peak value is the value of relative intensity corresponding to a frequency of 1.0. Also indicated is the half-maximum (frequency = 0.5) position at which width was measured for statistical comparisons. Area is computed as the peak times the width. These two histograms were chosen because their peak and width values are closest to the mean values; however, there was large variation in shapes of the histograms. (*D*) Bar chart showing the difference between three descriptors of histograms from xDuctin- and KCNE1-injected embryos. Control xDuctin-injected histograms had a mean peak at 0.255 ± 0.093 (mean ± 99% confidence intervals), a mean width of 0.150 ± 0.042, and a mean area of 0.044 ± 0.030, whereas the mean peak for KCNE1-injected embryos was at 0.786 ± 0.134, the mean width was 0.627 ± 0.192, and mean area was 0.552 ± 0.308. Two-tailed t tests revealed highly significant differences for each comparison: peaks, $P = 8 \times 10^{-10}$; widths, $P = 2 \times 10^{-6}$; areas, $P = 4 \times 10^{-4}$. Control n = 15; KCNE1 n = 22.

Consistent with this and with the inhibition of KCNQ1 function by KCNE1, analysis using the fluorescent membrane voltage reporter dye DiSBAC (28) revealed that embryonic cells were significantly depolarized by KCNE1 injection. Although it is not yet possible to calibrate DiSBAC fluorescence changes to absolute millivolt values, analysis of the data clearly showed (Fig. 2 *C* and *D*) that transmembrane potential is significantly depolarized by KCNE1 mRNA injection but not by injection of a control mRNA (encoding an ion transporter that does not inhibit polarizing currents). We conclude that the embryonic effects of KCNE1 are likely to be mediated by its inhibitory effect on KCNQ1 activity and the resulting cellular depolarization.

KCNE1 Expression Alters Proliferation, Migration, and Invasiveness of Melanocytes. We then characterized the phenotype further, noting that melanocytes not only were greater in number but also were

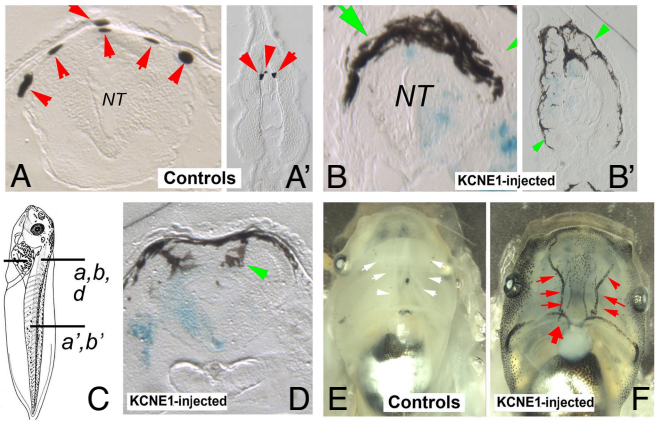

Fig. 3. KCNE1 expression induces a neoplastic-like phenotype in melanocytes. Control larvae sectioned through the brain (*A*) and tail (*A′*) possess a small number of melanocytes at the dorsal surface of the neural tube (NT); these cells have the normal rounded morphology (red arrows). In contrast, embryos injected with KCNE1 exhibit higher numbers of melanocytes that spread out into a more dendritic morphology (green arrows), observed in both the brain (*B*) and the tail (*B′*, where the melanocytes penetrate the somite and surround the spinal cord). (*C*) The level of sections for *A*, *A′*, *B*, *B′*, and *D*. (*D*) Melanocytes of KCNE1-injected larvae often invade the dense nervous tissues of the neural tube (green arrow). Blue stain in *B*, *B′*, and *D* indicates lineage label coinjected with KCNE1 mRNA. At 3 months, the ectopic melanocytes colonized the blood vessels (control embryo in *E*, white arrows, vs. KCNE1-injected in *F*, red arrows). (Magnifications: *A*, *B*, and *D*, ×12; *A′* and *B′*, ×20; *E* and *F*, ×7.5.)

located in aberrant locations in the embryo. The ectopic melanocytes induced by KCNE1 exhibited a highly invasive character and a spread-out dendritic morphology characteristic of many metastatic cells. These cells colonized the neural tube, wrapping around the spinal cord and sending processes into the dense neural tissue (Fig. 3 *A*–*B′* and *D*). In contrast, the KCNQ1 opener drug RL-3 (29) caused 46% of the embryos to exhibit a lighter, hypopigmented phenotype compared with controls ($n = 28$), the effect being greater in the tail (Fig. S6 *A* and *A′*). The melanocytes continued spreading across the epidermal layers and were particularly attracted to ganglia, the gut, and organ primordia, colonizing them at high density; sometimes, tissue outgrowths were observed, with a presence of ectopic melanocytes in the center (Figs. S6 and S7). Ectopic melanocytes also colonized the blood vessels (Fig. 3 *E* and *F*), as observed in melanoma (30).

To analyze the proliferation phenotype, we characterized the effect of KCNE1 by immunohistochemistry with an antibody to phosphorylated histone 3B, a standard marker of cells in the G_2/M cell cycle transition (Table 2). The melanocyte-rich region in the center of the flank had almost twice the number of mitotic cells in KCNE1-injected larvae than in controls, indicating that the proliferative increase conferred by KCNE1 lasts for at least 7 days past induction of the neural crest. However, there was no significant difference in the number of proliferative cells in the ventral flank (largely devoid of melanocytes), indicating that KCNE1 misexpression does not induce a global (nonselective) up-regulation of mitotic potential. Although we did not observe discrete tumors bearing classical histoarchitecture changes indicative of cancer, taken together these data reveal a neoplastic-like phenotype conferred upon individual melanocytes by the KCNE1 overexpression. This phenotype includes a change in melanocyte shape (spread out with extended processes), hyperproliferation, and aggressive invasion into multiple deep tissues at significant distances from their source.

Table 2. Quantification of proliferative cells

	Control	KCNE1 injected	*P* (*t* test)
Central flank	10.7 ± 4.5	19 ± 9.5	0.0027
Ventral fin	11.5 ± 4.9	13.2 ± 6.3	0.49

Embryos at the one-cell stage were injected with KCNE1 mRNA. At stage 45, control and injected larvae ($n = 12$ in each set) were fixed and processed for immunohistochemistry with the H3P antibody to reveal mitotic cells. Positive signal was counted in regions indicated; counts are presented ± SD. KCNE1-injected embryos possessed 1.7-fold more proliferative cells in the melanocyte-rich central flank, but the difference in the number of cells in the dorsal fin was nonsignificant.

KCNE1 Induces Neural Crest/Tumor Regulator Gene Expression in a Non-Cell-Autonomous Manner. We next used molecular markers to examine how KCNE1 induces the coordinated changes in melanocyte behavior. Ectopic KCNE1 could be acting within the melanocytes themselves or could provide cues to melanocytes when it is expressed in other cell types. The hyperpigmentation could arise from a normal melanoblast population being forced through more rapid cell cycles, or through additional cells outside the normal melanocyte lineage being converted to a pigment cell type (K^+ transport modulation may exert effects mainly on cell cycle machinery or on lineage switches during embryonic differentiation).

Injections of XKCNE1 mRNA into dorsal, ventral, or vegetal regions never (0%, $n = 84$) resulted in ectopic staining of the *Xtrp-2* (31) melanocyte precursor marker (Fig S8 *A* and *B*). Thus, the hyperproliferation phenotype does not arise from recruitment of cells from alternative locations into the melanocyte lineage. However, ectopic melanocytes were often found in regions that had not been themselves targeted by KCNE1 (e.g., dorsal head hyperpigmentation after injection of KCNE1 mRNA into ventral blastomeres). This is likely due to colonization of these regions by melanocytes that originate in KCNE1-positive areas, since melanocytes are highly migratory (32). Analysis of a lineage label of cells receiving KCNE1 mRNA (made possible by the mosaic expression that results from mRNA injected at the one-cell stage) revealed the non-cell-autonomous nature of this effect: the majority of ectopic melanocytes had not themselves received the KCNE1 mRNA (lineage label in Fig. 4 *A* and *B*).

Crucially, KCNE1 produced efficient ectopic induction of *Sox10* (Fig. 4*C*), a regulator of neural crest progenitor specification into the melanocyte lineage (33), and of *Slug* (Fig. 4*D*), a member of the SNAIL family of zinc finger transcriptional repressors that controls neural crest development and proliferation (33, 34). In contrast, a number of control markers and determinants of other types of embryonic structures (including OTX2, anterior specification; XHE1, hatching gland; CG1, cement gland; and Pax6, eye field) were not up-regulated in any of the embryos injected with KCNE1 ($n > 41$ in all cases). Thus, KCNE1 misexpression is able to selectively alter the spatial expression of at least two important regulators of neural crest lineages. Nevertheless, the dorsoanterior development, craniofacial patterning, and marker expression in the embryos and of the resulting larvae were normal, revealing that this effect is not inducing major alterations of head or heart morphogenesis (as would be expected if large numbers of cells were diverted from other neural crest lineages or if major and nonspecific changes in signaling factor expression were being caused). These data reveal that KCNE1 misexpression induces ectopic expression of powerful regulators of both neural crest and neoplastic cell behavior (35–38).

Discussion

Gain-of-function experiments have demonstrated that artificial modulation of endogenous bioelectrical events can provide signals altering morphogenesis and cell behavior in a coherent, spatially instructive manner (2). It has been suggested that three-dimensional systems of voltage gradients may be coordinates for cell migration and morphogenesis (39, 40), and neural crest is particularly sensitive to extracellular electrical cues (41). However, in most cases the molecular details of these events remain unknown.

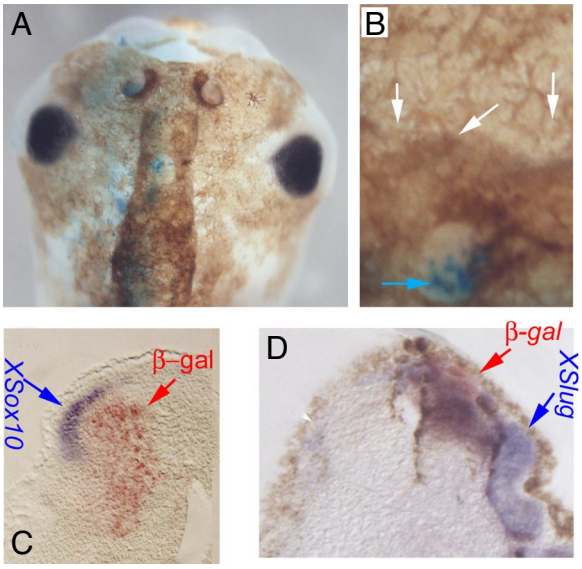

Fig. 4. KCNE1-induced hyperpigmentation phenotype is a non-cell-autonomous effect involving up-regulation of *Sox10* and *Slug* expression. (*A*) Embryos were injected with a mixture of KCNE1 and β-gal mRNAs and were lightly bleached at stage 43, allowing evaluation of melanocytes and clear detection of the β-gal lineage label in the area dorsal to the eyes, which normally has few or no melanocytes (all of the melanocytes in this region are ectopic). The vast majority of the excess cells did not themselves contain the lineage label (*B*, white arrows indicate lack of β-gal signal; blue arrow indicates cells positive for β-gal), illustrating the non-cell-autonomous mechanism of hyperpigmentation induction by KCNE1. Embryos were injected with KCNE1 + β-gal mRNAs at the one-cell stage (resulting in mosaic expression throughout the embryo), processed for *in situ* hybridization, and sectioned. Note the ectopic expression of *Sox10* (*C*) and *Xslug* (*D*, compare with contralateral side showing very little *Sox10* expression on the side where KCNE1 was not injected). Ectopic domains lie adjacent to KCNE1-misexpressing cells. Red signal (and red arrowheads) indicate β-gal lineage label of injected cells. Blue arrows indicate the positive *in situ* hybridization signal (purple).

In particular, the least is known about how ion flows regulate embryonic stem cell functions, and what downstream transcriptional targets couple bioelectrical events to specific cell behaviors. Our data identify KCNQ/KCNE1 complexes as a fascinating example of the genetic underpinning of such biophysical signals.

Misexpression of wild-type KCNE1 induces a striking phenotype caused by overproliferation of melanocytes. Other cell types may have been affected, but the embryos exhibited very normal development of most structures (including neural crest derivatives, such as heart and craniofacial structures). Moreover, the proliferative effect was not detected in melanocyte-poor regions of KCNE1-injected larvae (Table 2). Thus, the phenotype is not a broad misregulation of embryonic proliferation, migration, or differentiation, but rather affects primarily one (or a small number) of embryonic cell types.

Direct, specific pharmacological activation and blockade of KCNQ1 by RL-3 and Chromanol 293B reduced and increased, respectively, the pigmentation of larvae. Misexpression of MiRP2 (a regulatory subunit in the KCNE family that suppresses ERG channels) or other K^+ channel subunits did not induce hyperpigmentation. Thus, independent confirmation using molecular genetic and pharmacological techniques implicates KCNQ1 as the proximal target of KCNE1 misexpression and implicates KCNQ1 in the control of melanocyte behavior.

The data suggest an inhibitory role for KCNE1 on KCNQ1 activity. Our direct electrophysiology results show that although KCNQ1 contributes significantly to membrane potential, coexpression of KCNE1 suppresses KCNQ1 channel currents (without detectable alterations of KCNQ1 channel proteins at the plasma membrane) and depolarizes embryonic cells *in vivo*. Misexpression of MiRP2 (which does not inhibit KCNQ1 function at any potential) does not induce hyperpigmentation. KCNE1's decrease of KCNQ1's current at physiological potential explains why KCNE1 overexpression and KCNQ1 blockade affect melanocytes in the same way; the reduction of KCNQ1 currents by KCNE1 expression is also consistent with our direct observation of depolarization induced by KCNE1. Given the known presence of voltage gradients in embryos (42), it is clear that future efforts to understand control of neural crest, and stem cell behavior in general, must take into account membrane potentials and ion flows in these cells and their niche. Importantly, although an association between depolarization and up-regulation of proliferation has been suggested previously (43), the induction of hyperproliferation by KCNE1-mediated depolarization provides molecular evidence for a functional role of membrane potential in mitotic regulation.

Marker analysis showed that the effect of KCNE1 is on the endogenous set of melanocyte precursors and does not entail conversion of cells from unrelated regions into melanocyte fate. The normal craniofacial patterning and cardiovascular function (two sensitive readouts) suggest that other neural crest derivatives have not been diverted from their normal migration or respecified into pigment cells by KCNE1. Rather than altering specification, KCNE1 misexpression induces long-lasting increases in cell proliferation rate and changes in cell shape. Because *XSox10* and *XSlug* are necessary and sufficient for the hyperproliferation of melanocytes (33, 44), the up-regulation of these targets by KCNE1 misexpression accounts for the observed phenotypes. Although it is possible that other genes also were activated by the changes in membrane potential, a global nonspecific effect is ruled out by the normal development of the KCNE1-injected animals. The data implicating up-regulation of *Sox10* and *Slug* provide a unique example of the identification of transcriptional target readouts of non-cell-autonomous ion channel modulation effects and provide a powerful model for studies to molecularly dissect steps leading from depolarization to the activation of key transcription factors.

Our results suggest a model for the role of KCNE1 in modulating the behavior of the melanocyte neural crest lineage during embryonic development (Fig. 5): expression of KCNE1 reduces KCNQ1 function, depolarizing cells and leading to the up-regulation of *XSox10* and its downstream targets, such as *Xslug* in neighboring cells, inducing their proliferation and invasiveness.

This role for KCNQ1/KCNE1 in regulating cell proliferation may have implications for cancer biology, since a number of "channelopathies" have been suggested to contribute to neoplasm (3, 45). Significant correlations have been found between neoplastic potential and bioelectrical properties of cells (45–49). These biophysical properties are not simply markers but are functional signals; misexpression of an ion transporter induces tumorigenicity in fibroblasts (50), and inhibition of EAG channel function suppresses neoplasm in an animal model *in vivo* (51). Ion channel function controls the proliferation rate and invasiveness of a number of cell types that often form tumors (49, 52–55), and overexpression of KCNK9 (strongly overexpressed in breast cancer) promotes tumor formation and confers resistance to hypoxia and serum deprivation (56). Misexpression of KCNE1 did not induce tumors *per se*. However, KCNE1 misexpression conferred several properties on melanocytes that are strongly associated with cancer cells (e.g., melanoma; ref. 57): up-regulation of *Sox10* and *Slug*, hyperproliferation, increased dendricity, invasive colonization of a wide range of organs and tissues (blood vessels and neural tube), and ectopic growths. SLUG not only is a critical regulator of neural crest development (44) but also has been implicated in the acquisition of invasive behavior, increase of proliferation, and maintenance of neoplastic phenotype during tumor progression (58).

It is unknown whether KCNE1-dependent mechanisms are relevant to any clinical cancers. However, taken together, the five

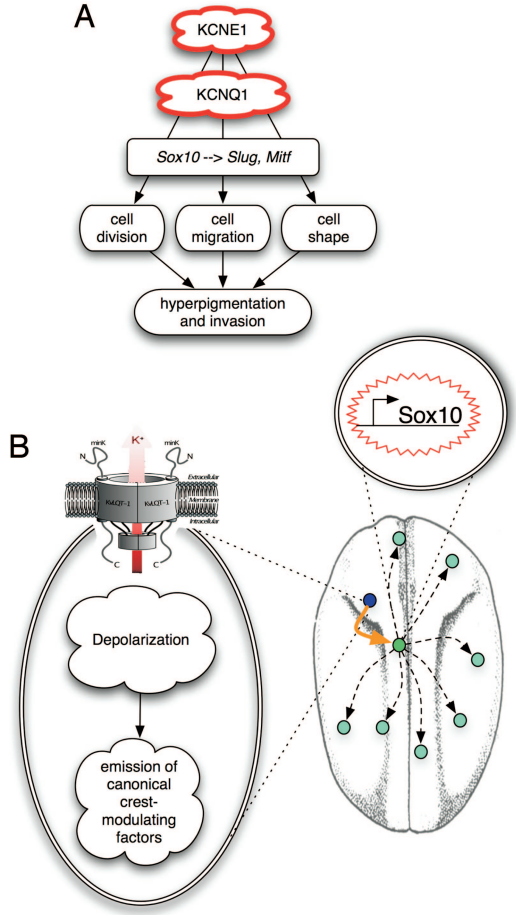

Fig. 5. A model of KCNQ1/KCNE1 function in embryogenesis. (*A*) A parsimonious model of the data proposes that KCNE1 modifies the function of KCNQ1, which up-regulates *Sox10* and its downstream targets, such as *XSlug*. These factors are known to be necessary and sufficient for the observed up-regulation of proliferation, change in cell shape, and induction of invasive migration behavior in melanocytes. (*B*) Embryonic regions expressing KCNE1 induce up-regulation of key transcription factors, such as *Sox10* and *Slug,* in other cells in the neural crest population, which confers upon them a hyperproliferative, invasive phenotype. This illustrates a non-cell-autonomous mechanism by which ion flows are transduced into canonical transcription cascades that control cell behavior. Black dashed lines indicate migration of hyperproliferating offspring of the target (green) cell. The original event takes place in the cell expressing KCNE1 (blue), which does not itself contribute all of the proliferative offspring. The target cell may induce the *XSox10* pathway in neighbors by conventional biochemical signals (e.g., BMPs, FGFs, and WNTs). The direct biophysical interaction occurs in the target cell, where KCNE1-mediated loss of membrane polarization is relayed to the downstream signaling machinery by cell-autonomous mechanisms.

phenotypes arising from KCNE1 expression demonstrate that changes in bioelectrical signals can confer neoplastic-like properties on a specific embryonic stem cell population. The results of late Chromanol 293B exposure also show that mature neural crest cells or their derivatives (not only early crest populations) can be affected by K^+ channel modulation. In light of the conservation of molecular mechanisms, such as the Wnt and PTEN pathways in both stem cell regulation and neoplasia, the idea has been put forward that some cancers arise from misregulation of stem cell control (59–64). Because of the known role of bioelectric properties in neoplasia and the control of differentiation, proliferation, and migration in embryonic and adult cells, it is tempting to speculate that KCNE1/KCNQ1 is a biophysical environmental signal that shifts embryonic stem cells toward a neoplasia-like behavior.

The ubiquitous use of bioelectric mechanisms across phyla suggests that the KCNE1 phenotype may be of broad significance. KCNE1 roles have not been directly tested in mammalian neural crest function, although a microarray analysis (65) recently identified KCNQ1 as being up-regulated more than 3-fold in mice with an increased number of neural progenitor cells. The high conservation of *Sox10/Slug* signaling among vertebrates suggests that overexpression of KCNE1 should be investigated as a possible marker of (and a potentiating factor in) human metaplasia and neural crest defects.

Bioelectric events are a poorly understood form of "epigenetic" processes, which are of high significance in understanding cellular controls (66, 67). Our data implicate a clinically relevant ion channel protein in the orchestration of gene expression, cell number, shape, and location during development. Understanding the regulation of stem cell populations by the biophysical properties of the plasma membrane and extracellular ion flows will ultimately reveal novel markers and control points for biomedical intervention.

Methods

See *SI Methods* for additional details.

Expression Analysis. *In situ* hybridization was performed as in Harland (68) by using clones (24) for KCNQ1 (EF07869) and KCNE1 (AF545500). Immunohistochemistry was performed as in Levin (69) by using a polyclonal antibody to IsK (70) at 1:1,000 and KCNQ1 antibodies generated by Invitrogen to peptide sequences TYEQLNVPRMTQDNIS and ITHISELKEHHRAAIK (1:500).

Microinjection. Capped, synthetic mRNAs (≈2.7 nl) were dissolved in water and injected into embryos in 3% Ficoll. Results of injections are reported as percentage of otherwise normal embryos that were hyperpigmented, sample size (*n*), and *P* values comparing treated groups to controls.

Electrophysiology. Whole-cell currents in *Xenopus* oocytes were recorded with standard two-electrode voltage-clamp techniques. Data were acquired with Clampex (pCLAMP 8.0, Axon Instruments) and analyzed with ClampFit (pCLAMP 8.0, Axon Instruments) and Origin 6.0 (Microcal). Whole-cell currents were recorded in ND96 solution (see *SI Methods*).

Imaging of Membrane Voltage Patterns by Using DiSBAC$_2$(3). Fresh DiSBAC (Molecular Probes) stocks (stock = 1 mg/ml in DMSO) were diluted 1:10 in distilled water; that primary dilution then was diluted 1:1000 in 0.1× Modified Marc Ringer's solution for a final concentration of 0.2 μM. Stage 20–24 embryos were soaked in dye for 30 min. Embryos in solution were imaged using the TRITC cube set on an Olympus BX61 microscope with an ORCA digital CCD camera (Hamamatsu) with IPLabs software. Each embryo was brought into focus, the milliseconds of exposure were set, and the image was taken. Before imaging the next embryo, the contents of the Petri dish were swirled to ensure even distribution of dye.

Images were segmented by hand such that the entire image of the embryo was defined as the region of interest. IPLabs software then generated histograms of the distribution of pixel intensities within the region of interest. Frequencies were normalized to maximum frequency to correct for different numbers of pixels measured. Intensities were converted from 0 to 4095 to 0 to 255 by IPLabs. Because different exposures were required for different embryos, intensity values then were normalized to milliseconds of exposure. We characterized the resulting distributions (histograms, see Fig. 2*C*) by comparing the mean width of the first peak at half-maximum (Fig. 2*D*).

ACKNOWLEDGMENTS. We thank Punita Koustubhan and Amber Currier for *Xenopus* husbandry; Dayong Qiu for general lab assistance; Drucilla Roberts for help with pathohistology; Harry Witchel, Michael Sanguinetti, and Uwe Gerlach for advice on KCNQ1 physiology and pharmacology; Michael Schwake for RL-3; Jaques Barhanin for KCNE1 antibody; Naoto Ueno and Takamasa Yamamoto for EST clones; Geoffrey Abbott for the MiRP2 clone; Roberto Mayor and Michael Klymkowski for information on neural crest anatomy; Kelly McLaughlin, Wendy Beane, and Laura Vandenberg for comments on the manuscript; Kristin Artinger, Yun Kee, and Carole LaBonne for advice and *in situ* probe; and Peter Smith and the BioCurrents Research Center for support and discussions. This work was supported by grants to M.L. from the National Institutes of Health (R01-GM07742), American Heart Association (0740088N), National Highway Traffic Safety Administration (DTNH22-06-G-00001), and March of Dimes (6-FY04-65), and by National Institutes of Health Grants 5T32DE007327-07 (to D.B.) and 5K22DE16633 (to D.S.A.).

1. McCaig CD, *et al.* (2005) Controlling cell behavior electrically: Current views and future potential. *Physiol Rev* 85:943–978.
2. Levin M (2007) Large-scale biophysics: Ion flows and regeneration. *Trends Cell Biol* 17:262–271.
3. Kunzelmann K (2005) Ion channels and cancer. *J Membr Biol* 205:159–173.
4. Adams DS, *et al.* (2006) Early, H^+-V-ATPase-dependent proton flux is necessary for consistent left-right patterning of non-mammalian vertebrates. *Development* 133:1657–1671.
5. Zhao M, *et al.* (2006) Electrical signals control wound healing through phosphatidyl-inositol-3-OH kinase-gamma and PTEN. *Nature* 442:457–460.
6. Cone CD, Cone CM (1976) Induction of mitosis in mature neurons in central nervous system by sustained depolarization. *Science* 192:155–158.
7. Adams DS, Masi A, Levin M (2007) H^+ pump-dependent changes in membrane voltage are an early mechanism necessary and sufficient to induce Xenopus tail regeneration. *Development* 134:1323–1335.
8. Pineda RH, *et al.* (2006) Knockdown of Nav1.6a Na^+ channels affects zebrafish motoneuron development. *Development* 133:3827–3836.
9. Biagiotti T, *et al.* (2006) Cell renewing in neuroblastoma: Electrophysiological and immunocytochemical characterization of stem cells and derivatives. *Stem Cells* 24:443–453.
10. Bai X, *et al.* (2007) Electrophysiological properties of human adipose tissue-derived stem cells. *Am J Physiol Cell Physiol* 293:C1539–C1550.
11. Cai J, *et al.* (2004) Membrane properties of rat embryonic multipotent neural stem cells. *J Neurochem* 88:212–226.
12. Wong RC, *et al.* (2004) Presence of functional gap junctions in human embryonic stem cells. *Stem Cells* 22:883–889.
13. Tazuke SI, *et al.* (2002) A germline-specific gap junction protein required for survival of differentiating early germ cells. *Development* 129:2529–2539.
14. van Kempen M, *et al.* (2003) Expression of the electrophysiological system during murine embryonic stem cell cardiac differentiation. *Cell Physiol Biochem* 13:263–270.
15. Konig S, *et al.* (2004) Membrane hyperpolarization triggers myogenin and myocyte enhancer factor-2 expression during human myoblast differentiation. *J Biol Chem* 279:28187–28196.
16. Harrington DB (1972) Electrical stimulation of RNA and protein-synthesis in frog erythrocyte. *Anat Rec* 172:325.
17. Harrington DB, Becker RO (1973) Electrical stimulation of RNA and protein synthesis in the frog erythrocyte. *Exp Cell Res* 76:95–98.
18. Aw S, *et al.* (2008) H,K-ATPase protein localization and Kir4.1 function reveal concordance of three axes during early determination of left-right asymmetry. *Mech Dev* 125:353–372.
19. Levin M, *et al.* (2002) Asymmetries in H^+/K^+-ATPase and cell membrane potentials comprise a very early step in left-right patterning. *Cell* 111:77–89.
20. Barhanin J, *et al.* (1996) K(V)LQT1 and IsK (minK) proteins associate to form the I(Ks) cardiac potassium current. *Nature* 384:78–80.
21. Sanguinetti M, *et al.* (1996) Coassembly of K(V)LQT1 and minK (IsK) proteins to form cardiac I(Ks) potassium channel. *Nature* 384:80–83.
22. Wang Q, *et al.* (1996) Positional cloning of a novel potassium channel gene: KVLQT1 mutations cause cardiac arrhythmias. *Nat Genet* 12:17–23.
23. Casimiro MC, *et al.* (2001) Targeted disruption of the Kcnq1 gene produces a mouse model of Jervell and Lange–Nielsen Syndrome. *Proc Natl Acad Sci USA* 98:2526–2531.
24. Morokuma J, Blackiston D, Levin M (2008) KCNQ1 and KCNE1 K^+ channel components are involved in early left-right patterning in Xenopus laevis embryos. *Cell Physiol Biochem* 21:345–360.
25. Maljevic S, Wuttke TV, Lerche H (2008) Nervous system KV7 disorders: Breakdown of a subthreshold brake. *J Physiol* 586:1791–1801.
26. Peroz D, *et al.* (2008) Kv7.1 (KCNQ1) properties and channelopathies. *J Physiol* 586:1785–1789.
27. Bleich M, *et al.* (1997) KVLQT channels are inhibited by the K^+ channel blocker 293B. *Pflügers Arch* 434:499–501.
28. Adams DS, Levin M (2006) in *Analysis of Growth Factor Signaling in Embryos*, eds Whitman M, Sater AK (Taylor and Francis, Boca Raton, FL), pp 177–262.
29. Salata JJ, *et al.* (1998) A novel benzodiazepine that activates cardiac slow delayed rectifier K^+ currents. *Mol Pharmacol* 54:220–230.
30. Velazquez OC, Herlyn M (2003) The vascular phenotype of melanoma metastasis. *Clin Exp Metastasis* 20:229–235.
31. Kumasaka M, *et al.* (2003) Isolation and developmental expression of tyrosinase family genes in Xenopus laevis. *Pigment Cell Res* 16:455–462.
32. Wilson HC, Milos NC (1987) The effects of various nutritional supplements on the growth, migration and differentiation of Xenopus laevis neural crest cells in vitro. *In Vitro Cell Dev Biol* 23:323–331.
33. Aoki Y, *et al.* (2003) Sox10 regulates the development of neural crest-derived melanocytes in Xenopus. *Dev Biol* 259:19–33.
34. Turner FE, *et al.* (2006) Slug regulates integrin expression and cell proliferation in human epidermal keratinocytes. *J Biol Chem* 281:21321–21331.
35. Martin TA, *et al.* (2005) Expression of the transcription factors snail, slug, and twist and their clinical significance in human breast cancer. *Ann Surg Oncol* 12:488–496.
36. Kurrey NK, Amit K, Bapat SA (2005) Snail and Slug are major determinants of ovarian cancer invasiveness at the transcription level. *Gynecol Oncol* 97:155–165.
37. Khong HT, Rosenberg SA (2002) The Waardenburg syndrome type 4 gene, *SOX10*, is a novel tumor-associated antigen identified in a patient with a dramatic response to immunotherapy. *Cancer Res* 62:3020–3023.
38. Ferletta M, *et al.* (2007) Sox10 has a broad expression pattern in gliomas and enhances platelet-derived growth factor-B-induced gliomagenesis. *Mol Cancer Res* 5:891–897.
39. Shi R, Borgens RB (1995) Three-dimensional gradients of voltage during development of the nervous system as invisible coordinates for the establishment of embryonic pattern. *Dev Dyn* 202:101–114.
40. Hotary KB, Robinson KR (1994) Endogenous electrical currents and voltage gradients in Xenopus embryos and the consequences of their disruption. *Dev Biol* 166:789–800.
41. Stump RF, Robinson KR (1983) Xenopus neural crest cell migration in an applied electrical field. *J Cell Biol* 97:1226–1233.
42. Nuccitelli R, Robinson K, Jaffe L (1986) On electrical currents in development. *BioEssays* 5:292–294.
43. Cone CD, Tongier M (1971) Control of somatic cell mitosis by simulated changes in the transmembrane potential level. *Oncology* 25:168–182.
44. Carl TF, *et al.* (1999) Inhibition of neural crest migration in Xenopus using antisense slug RNA. *Dev Biol* 213:101–115.
45. Fraser SP, *et al.* (2005) Voltage-gated sodium channel expression and potentiation of human breast cancer metastasis. *Clin Cancer Res* 11:5381–5389.
46. Burr HS, Langman L (1949) Electronegativity of the cancerous cervix - reply. *Am J Obstet Gynecol* 58:414–414.
47. Killion JJ (1984) Electrical properties of normal and transformed mammalian cells. *Biophys J* 45:523–528.
48. Martinez-Zaguilan R, *et al.* (1993) Vacuolar-type H^+-ATPases are functionally expressed in plasma membranes of human tumor cells. *Am J Physiol* 265:C1015–C1029.
49. Arcangeli A, *et al.* (1995) A novel inward-rectifying K^+ current with a cell-cycle dependence governs the resting potential of mammalian neuroblastoma cells. *J Physiol* 489:455–471.
50. Perona R, Serrano R (1988) Increased pH and tumorigenicity of fibroblasts expressing a yeast proton pump. *Nature* 334:438–440.
51. Pardo LA, *et al.* (1999) Oncogenic potential of EAG K^+ channels. *EMBO J* 18:5540–5547.
52. Pillozzi S, *et al.* (2002) HERG potassium channels are constitutively expressed in primary human acute myeloid leukemias and regulate cell proliferation of normal and leukemic hemopoietic progenitors. *Leukemia* 16:1791–1798.
53. Wang S, *et al.* (1998) Evidence for an early G1 ionic event necessary for cell cycle progression and survival in the MCF-7 human breast carcinoma cell line. *J Cell Physiol* 176:456–464.
54. Knutson P, *et al.* (1997) K^+ channel expression and cell proliferation are regulated by intracellular sodium and membrane depolarization in oligodendrocyte progenitor cells. *J Neurosci* 17:2669–2682.
55. Klimatcheva E, Wonderlin W (1999) An ATP-sensitive K^+ current that regulates progression through early G1 phase of the cell cycle in MCF-7 human breast cancer cells. *J Membr Biol* 171:35–46.
56. Mu D, *et al.* (2003) Genomic amplification and oncogenic properties of the KCNK9 potassium channel gene. *Cancer Cell* 3:297–302.
57. Miyazaki K (2004) Novel approach for evaluation of estrogenic and anti-estrogenic activities of genistein and daidzein using B16 melanoma cells and dendricity assay. *Pigment Cell Res* 17:407–412.
58. Hotz B, *et al.* (2007) Epithelial to mesenchymal transition: Expression of the regulators snail, slug, and twist in pancreatic cancer. *Clin Cancer Res* 13:4769–4776.
59. Li Y, *et al.* (2003) Evidence that transgenes encoding components of the Wnt signaling pathway preferentially induce mammary cancers from progenitor cells. *Proc Natl Acad Sci USA* 100:15853–15858.
60. Howard B, Ashworth A (2006) Signalling pathways implicated in early mammary gland morphogenesis and breast cancer. *PLoS Genet* 2:e112.
61. Lindvall C, *et al.* (2006) The Wnt signaling receptor Lrp5 is required for mammary ductal stem cell activity and Wnt1-induced tumorigenesis. *J Biol Chem* 281:35081–35087.
62. Hong D, *et al.* (2008) Initiating and cancer-propagating cells in TEL-AML1-associated childhood leukemia. *Science* 319:336–339.
63. Bjerkvig R, Tysnes BB, Aboody KS, Najbauer J, Terzis AJ (2005) Opinion: The origin of the cancer stem cell: Current controversies and new insights. *Nat Rev Cancer* 5:899–904.
64. Reya T, *et al.* (2001) Stem cells, cancer, and cancer stem cells. *Nature* 414:105–111.
65. Shi J, *et al.* (2007) Injury-induced neurogenesis in Bax-deficient mice: Evidence for regulation by voltage-gated potassium channels. *Eur J Neurosci* 25:3499–3512.
66. Jaffe LF (2003) Epigenetic theories of cancer initiation. *Adv Cancer Res* 90:209–230.
67. Ducasse M, Brown MA (2006) Epigenetic aberrations and cancer. *Mol Cancer* 5:60.
68. Harland RM (1991) in *Xenopus laevis: Practical Uses in Cell and Molecular Biology*, eds Kay BK, Peng HB (Academic, San Diego), pp 685–695.
69. Levin M (2004) A novel immunohistochemical method for evaluation of antibody specificity and detection of labile targets in biological tissue. *J Biochem Biophys Methods* 58:85–96.
70. Lesage F, *et al.* (1993) Are Xenopus oocytes unique in displaying functional IsK channel heterologous expression? *Receptors Channels* 1:143–152.